PHYSICAL REVIEW B **85**, 094430 (2012)

Spin-orbit effects in heavy-atom organic radical ferromagnets

Stephen M. Winter and Richard T. Oakley*
Department of Chemistry, University of Waterloo, Waterloo, Ontario, Canada N2L 3G1

Alexey E. Kovalev and Stephen Hill†
National High Magnetic Field Laboratory and Department of Physics, Florida State University, Tallahassee, Florida 32310 USA

(Received 13 January 2012; published 27 March 2012)

We discuss the effects of the spin-orbit interaction on heavy-atom organic magnets with specific reference to a series of isostructural sulfur- and selenium-based radical ferromagnets of tetragonal space group $P\bar{4}2_1m$. By using a perturbative approach, we show the spin-orbit effects lead to a pairwise anisotropic exchange interaction between neighboring radicals that provides an easy magnetic axis running parallel to the c-axis. Estimates of the magnitude of this magnetic anisotropy explain the significant increase in the coercive fields by virtue of selenium incorporation. Complementing this theoretical discussion are the results of ferromagnetic resonance studies, which provide an experimental verification of both the magnitude and symmetry of the spin-orbit terms. Taken as a whole, the results underscore the importance of heavy atoms and crystal symmetry in the design of molecular ferromagnets with large magnetic anisotropy and high ordering temperatures.

DOI: 10.1103/PhysRevB.85.094430 PACS number(s): 76.50.+g, 75.30.Gw, 71.70.Ej, 75.10.Dg

I. INTRODUCTION

The design of ferromagnetic materials has traditionally relied on the use of d- and f-block elements. The discovery 20 years ago of ferromagnetic ordering in light atom p-block (N, O) radicals appeared to provide a major conceptual advance, suggesting a new era in nonmetal molecular magnetism.[1–4] However, the weak through-space magnetic exchange interactions present in these materials afforded very low Curie temperatures T_C (<2 K), and the localization of spin density on light atoms (low Z) ensured a low magnetic anisotropy. As a result, the coercive fields H_c observed never exceeded a few Oersted.[5] Although novel, the weak response of these light-atom ferromagnets confirmed rather than challenged the "metals only" approach to magnetic materials. In this context, the recent report of ferromagnetic ordering in the heavy-atom (high-Z) bisdiselenazolyl radical **1**, which displays a T_C of 17 K and a coercive field H_c (at 2 K) of 1370 Oe, has reopened the debate on the possibility of nonmetal-based ferromagnetism.[6] The key question to address is the role of the heavy atom in the increase in T_C and H_c values of Se-based radicals relative to those seen in light-atom ferromagnets.

Radical **1** is the heaviest of a family of four sulfur- and selenium-based variants **1**–**4**, all of which crystallize in the noncentric tetragonal space group $P\bar{4}2_1m$. The crystal structures (Fig. 1) consist of pinwheel-like clusters of radicals arranged about $\bar{4}$ centers, with each radical providing the basis for a slipped π-stack array running parallel to the c-axis. The fact that all four materials are isostructural offers a unique opportunity to study the effect of S/Se incorporation. For example, the presence of the heavier chalcogen is crucial for achieving a high magnetic ordering temperature. There is no evidence for magnetic ordering, to date, in the purely sulfur-based material **4**.[7] The mixed S/Se variant **2** orders ferromagnetically, although its T_C (13 K) and H_c (250 Oe at 2 K) are less than that observed for the all-selenium radical **1**.[8,9] The other mixed S/Se system **3** also orders, although as a spin-canted antiferromagnet, with $T_N = 14$ K.[7] The increase in ordering temperature with Se incorporation can be

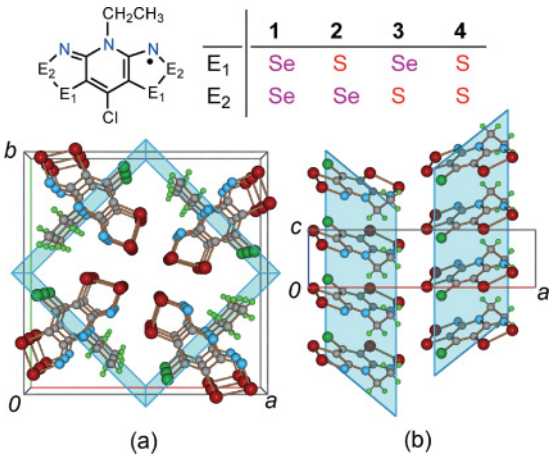

FIG. 1. (Color online) Crystal packing of **1** viewed (a) parallel and (b) perpendicular to the π-stacking direction, the crystallographic c-axis. Radicals **1**–**4** are isostructural. The positions of the crystallographic mirror planes are indicated in blue.

partly understood in terms of an enhancement of the isotropic exchange interactions occasioned by more diffuse magnetic orbitals.[10] The increase in H_c has been associated with an enhancement of anisotropic exchange interactions resulting from spin-orbit effects.[11]

In order to explore the role of spin-orbit effects in this series, we present a theoretical framework for understanding the magnitude and symmetry of the anisotropic exchange terms. While the results of this analysis relate directly to the properties of molecular p-block magnets, they are of equal relevance to more conventional d- and f-electron systems. The theoretical arguments are complemented by the results of ferromagnetic resonance (FMR) experiments on **1** and **2**, which have allowed detailed insight into the magnetic anisotropy in their ordered phase. Both **1** and **2** exhibit a zero-field gap in the resonance frequency that is several orders of magnitude larger than that observed in light-atom ferromagnets, and consistent with the presence of easy-axis magnetic anisotropy. These observations are shown to be in good agreement with

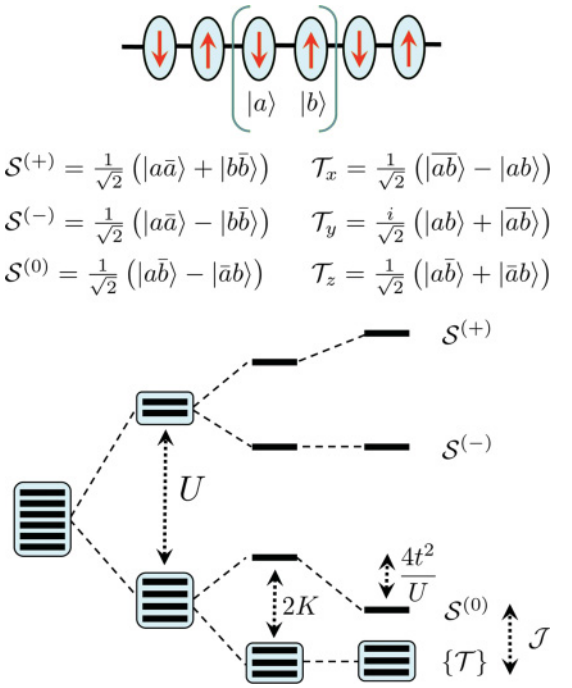

FIG. 2. (Color online) Splitting of the three singlet and triplet states arising from the two-site, two-orbital treatment of a lattice of interacting $S = \frac{1}{2}$ radicals. U represents the onsite Coulomb repulsion, t is the charge transfer or hopping integral, and K is the electronic exchange integral. The singlet-triplet energy gap is defined such that the exchange coupling constant $\mathcal{J} = \Delta E_{ST}$. The notation $|a\bar{b}\rangle$ denotes a state with an $m_s = +\frac{1}{2}$ in orbital a, and $m_s = -\frac{1}{2}$ in orbital b.

the anticipated symmetry and magnitude of the anisotropic exchange terms.

II. MAGNETIC HAMILTONIAN

Organic radicals have been studied extensively for many years, with a view to harnessing their unpaired electrons to serve as charge carriers and magnetic spins.[12–14] Historically, the incorporation of heavy atoms into radicals has been pursued in order to enhance conductivity by way of the more diffuse orbitals.[15] If one considers a lattice of radicals, each with one unpaired electron, the electronic and magnetic structure of the resulting array can be conveniently understood with reference to the Hubbard model.[16] When the intermolecular charge transfer or hopping integral t is large in comparison to the onsite Coulomb potential U, the material should possess a metallic ground state with a half-filled ($f = \frac{1}{2}$) band. However, despite steady progress in the design of materials with increased t/U ratios, a radical-based $f = \frac{1}{2}$ system displaying metallic properties has yet to be realized. Instead, for the resulting Mott insulating case when overlap is small compared to U, the unpaired electrons are localized, and the low-energy degrees of freedom are essentially magnetic.

The Hamiltonian that describes these magnetic degrees of freedom is typically discussed with specific reference to the two-site, two-orbital case shown in Fig. 2.[17] This configuration affords two charge-transfer singlet states $\mathcal{S}^{(+)}$ (in-phase) and $\mathcal{S}^{(-)}$ (out-of-phase), an open-shell singlet state $\mathcal{S}^{(0)}$, and

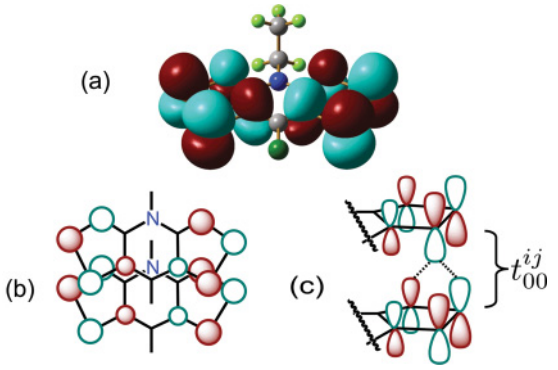

FIG. 3. (Color online) (a) UB3LYP/6-311G(d,p) Kohn-Sham isosurface for the A'' SOMO of **1**. (b) Schematic view of overlay of SOMOs on adjacent radicals along slipped π-stacks. (c) Near orthogonal overlap of neighboring SOMOs along the π-stack, leading to a small t_{00}^{ij} and thus a positive ferromagnetic exchange interaction $\mathcal{J}^{\pi}$.

a triplet manifold {$\mathcal{T}$}. The effect of the onsite Coulomb potential is to increase the energy of the charge-transfer states by U with respect to the open-shell states. Electronic exchange (or Hund's rule coupling) stabilizes the triplet with respect to the open-shell singlet $\mathcal{S}^{(0)}$ by $2K$ such that, in the absence of hopping, the two sites possess a triplet ground state. When hopping is included, there is a mixing of the in-phase charge-transfer singlet $\mathcal{S}^{(+)}$ with the open-shell singlet $\mathcal{S}^{(0)}$, lowering the energy of the latter by $4t^2/U$ at second order. As a result, the singlet-triplet energy gap $\Delta E_{ST} = \mathcal{J} = 2K - 4t^2/U$ and consequently the spin state of the two sites depends on the relative magnitude of K, t, and U. A ferromagnetic state is stabilized for small t/K ratios, i.e., positive $\mathcal{J}$ values. This observation is equivalent to the *orthogonal overlap* condition popularized by Kahn,[18,19] and employed extensively in the design of materials displaying ferromagnetic interactions.

The crystal architecture of **1**–**4** is such that the slipped π-stacked packing of radicals conforms almost perfectly to this prescription for ferromagnetism. The singly occupied molecular orbital (SOMO) is illustrated in Fig 3(a). The specific slippage of radicals along the π-stacks with respect to the stacking axis is such that the transfer integral between neighboring SOMOs (defined explicitly as t_{00}^{ij} below) is reduced to nearly zero [Figs. 3(b) and 3(c)].[10] As a result, the intrastack exchange interactions are expected to be ferromagnetic ($\mathcal{J}^{\pi} > 0$) for **1** and **2**. In conjunction with ferromagnetic interstack interactions, these considerations explain the ferromagnetically ordered ground state. The precariousness of the orthogonal overlap condition, however, is highlighted by the antiferromagnetic ordering of **3**, which differs from **1** and **2** only slightly in terms of slippage and internal bond lengths. Indeed, the ferromagnetic order can be destroyed by small changes in the degree of slippage either by chemical pressure, that is, through modification of the axial ligands,[9] or by the application of physical pressure.[20] While these arguments provide a satisfying rationalization of the isotropic magnetic interactions, it is our contention that a full understanding of the magnetic response of these systems requires the explicit inclusion of spin-orbit effects into the magnetic Hamiltonian.

Spin-orbit (SO) effects are incorporated by the addition of $\mathcal{H}_{SO} = \lambda\, \mathbf{L} \cdot \mathbf{S}$ to the nonrelativistic Hamiltonian, mixing

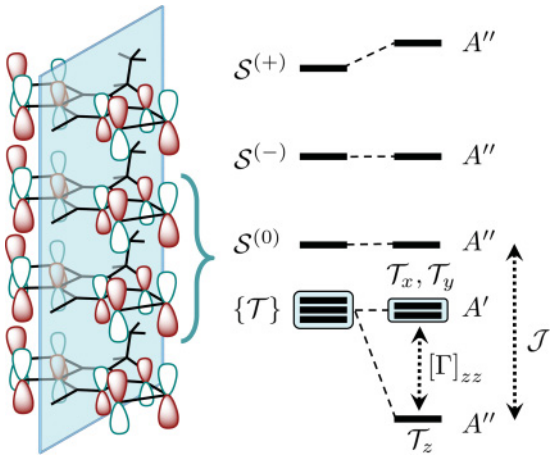

FIG. 4. (Color online) Spin-orbit splitting, for C_s symmetry, of the triplet manifold $\{\mathcal{T}\}$ in the two-site two-orbital case (continued from Fig. 2). The product of the spin and orbital symmetry is A' for $\mathcal{T}_x$ and $\mathcal{T}_y$ and A'' for $\mathcal{T}_z$. The splitting stabilizes the triplet with respect to the open-shell singlet $\mathcal{S}^{(0)}$ and provides the source of magnetic anisotropy.

states of pure **L** and **S**, while conserving the total angular momentum $\mathbf{J} = \mathbf{L} + \mathbf{S}$. The spin-orbit constant λ grows sharply with atomic number ($\lambda \propto Z^2$ to Z^4).[21] In the absence of SO coupling, isolated radicals possess a spin-doublet ground state with $L = 0$ and $S = \frac{1}{2}$. In the presence of SO coupling, the ground state is instead a $J = \frac{1}{2}$ doublet that is not a separate eigenstate of either $\mathbf{L}^2$ or $\mathbf{S}^2$. The effect of the spin-orbit coupling can be seen in the response of the resulting state to an external magnetic field $\mathbf{H}_{\text{ext}}$, which can be considered using an effective spin Hamiltonian $\mathcal{H} = \mathbf{H}_{\text{ext}} \cdot \mathbf{g} \cdot \mathbf{S}$. For historical reasons, the effective spin is written as **S** rather than being identified as **J**. The **g** tensor is often found to be quite anisotropic in heavy-atom radicals, indicating strong SO coupling.[22]

For such radicals, the spin-orbit effects may also lead to anisotropic magnetic interactions in the solid state. For the two-site case, in the absence of SO coupling, the isotropic magnetic interaction $\mathcal{H}_{\text{iso}} = -\mathcal{J}\ \mathbf{S}_i \cdot \mathbf{S}_j$ was shown to permit pure spin singlet $\mathcal{S}^{(0)}$ and triplet $\{\mathcal{T}\}$ eigenstates. In the general case, this interaction does not commute with the SO interaction, which admits singlet and triplet **J** states. When both are present, there are two consequences. First, the triplet manifold is split, an effect that is manifest as a magnetic anisotropy in ferromagnetic materials. Second, the eigenstates of the two-site model are not pure singlets or triplets of the effective spin; this effect is responsible for weak ferromagnetic moments in antiferromagnetic materials.

In reference to the two-site Hubbard model discussed above, the effect of spin-orbit coupling is to mix states of the triplet manifold $\{\mathcal{T}\}$ with the in-phase charge-transfer singlet $\mathcal{S}^{(+)}$ as shown in Fig. 4. By analogy with the stabilization of $\mathcal{S}^{(0)}$ due to hopping, the triplet state(s) capable of mixing are also lowered in energy at second order in λ, splitting the triplet manifold. Since both the open-shell singlet $\mathcal{S}^{(0)}$ and those triplet states are now mixed with the charge-transfer singlet $\mathcal{S}^{(+)}$, there is also a resultant mixing of the open-shell triplet and singlet states. This latter effect is the celebrated Dzyaloshinskii-Moriya (DM) interaction.

The states of the triplet manifold capable of mixing with the charge-transfer singlet are determined by the point group symmetry of the two sites, making symmetry an invaluable tool for investigating the magnetic effects of the spin-orbit interaction. It allows for the prediction of not only the specific splitting of the triplet manifold, but also the orientation of the canted moments in antiferromagnets. To demonstrate this, we provide two concrete examples. In the first case, the two sites are related by an inversion center, so that the minimum symmetry point group is C_i, which has two irreducible representations denoted A_g and A_u. It can be shown that the spin-orbit interaction can only mix states where the product of spin and orbital wave functions belongs to the same irreducible representation. In this case, the spin and orbital wave functions of $\mathcal{S}^{(+)}$ both belong to the A_g representation, resulting in a product $A_g \otimes A_g = A_g$. On the other hand, all the states in the triplet manifold have an orbital wave function of the A_u and spin wave functions of the A_g representation, with a product $A_u \otimes A_g = A_u$. For this specific case, therefore, no state in the triplet manifold is capable of mixing with $\mathcal{S}^{(+)}$ so that there is no splitting of the triplet manifold and no weak ferromagnetic moment. This result explains the rarity of spin canting for materials in centric space groups, but does not exclude the possibility.[23]

A second example, one that is directly applicable to **1** and **2**, is the case of mirror symmetry. Each molecule in a single π-stack is bisected by a mirror plane, making it appropriate to define molecular coordinates with respect to the local C_s symmetry: the z-axis is defined as normal to the mirror, and lies in the crystallographic ab-plane; the x-axis is aligned with the crystallographic c-axis, and the y-axis is chosen to form an orthogonal right-handed system (see Fig. 5). The C_s point group contains two irreducible representations: A', which is symmetric with respect to the mirror plane, and A'', which is antisymmetric. In this symmetry, the orbital wave function of all six states of the two-site model transforms as the same representation as the SOMO, that is, A''. The spin wave function of the charge-transfer singlet $\mathcal{S}^{(+)}$ transforms as A', resulting in a product $A'' \otimes A' = A''$. The spin wave functions of the states in the triplet manifold $\mathcal{T}_x$, $\mathcal{T}_y$, and $\mathcal{T}_z$ transform as A'', A'', and A', respectively. Therefore, only the $\mathcal{T}_z$ state of the triplet manifold has the correct symmetry to mix with the charge-transfer singlet. The interpretation of this result is that (a) for a ferromagnetic ground state, there is a preference for magnetization in the xy-plane of the molecules, and (b) for an antiferromagnetic ground state, the canted moment must lie in the xy-plane, as it arises directly from mixing $\mathcal{T}_z$ into the open-shell singlet. Although this approach of considering the total state symmetries provides an appealing qualitative view of the spin-orbit effects, a more convenient approach for quantitative analysis is provided below.

We will follow the approach first introduced by Moriya,[24] and later emphasized by Aharony *et al.*,[25] of first treating $\mathcal{H}_{\text{SO}}$ as a perturbation on the states of each single radical site before introducing hopping and Coulomb exchange. The magnetic interactions between radicals will then be considered, and shown to be anisotropic. As might be expected, the results of this approach agree qualitatively with results already described, but, in addition, will allow for the estimation of the magnitude of spin-orbit effects in terms of the parameters λ, t, and U.

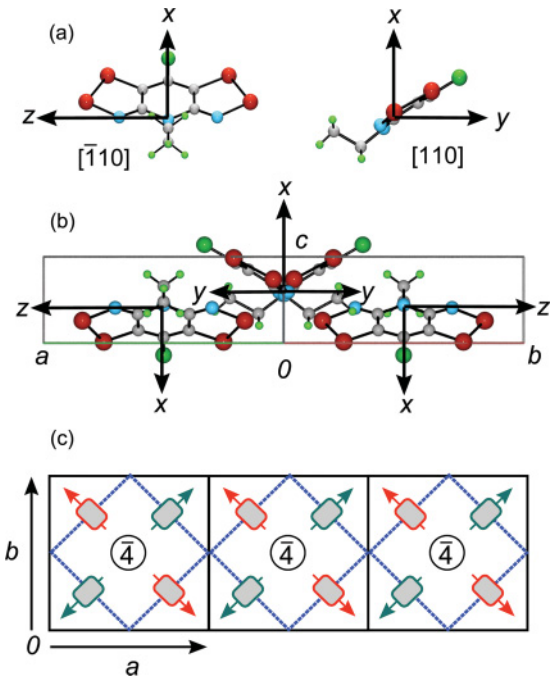

FIG. 5. (Color online) (a) Definition of local coordinate system of a single radical, viewed parallel to the [1̄10] and [110] directions. (b) Relative orientation of local coordinates of four radicals in the unit cell, viewed parallel to the [110] direction. (c) Anisotropic exchange terms viewed parallel to the [001] direction for three unit cells. Dashed blue lines indicate both the crystallographic mirror planes and the local easy xy-planes (see Fig. 1). The relative orientation of local $\mathbf{D}_{ij}$ vectors is indicated by an arrow along the local z-axis.

The convention used in this paper is to label unperturbed orbitals with roman characters and perturbed orbitals with the corresponding greek characters. In the unperturbed ground state of each radical, the highest occupied orbital is the singly occupied molecular orbital (SOMO, labeled $a = 0$). Each single-particle energy level is at least twofold degenerate owing to the degeneracy of $m_s = \pm\frac{1}{2}$ states. The effect of turning on the SO perturbation is to alter the single-particle energy levels through mixing of orbital and spin states:

$$|\alpha, m_j\rangle = |a, m_s\rangle + \lambda \sum_{b,m_s'} \frac{\langle b, m_{s'}|\mathbf{L}\cdot\mathbf{S}|a, m_s\rangle}{\epsilon_b - \epsilon_a}|b, m_{s'}\rangle + O(\lambda^2), \tag{1}$$

where $m_j = m_s$ and ϵ_a denotes the energy of the unperturbed a orbital. If the perturbation is small ($\lambda \ll \Delta\epsilon = \epsilon_b - \epsilon_a$), then the ordering of orbitals is unchanged in the perturbed ground state; the perturbed SOMO is obtained directly from its unperturbed counterpart. Each perturbed single-particle energy level is still at least doubly degenerate, with $m_j = \pm\frac{1}{2}$.

Moriya's results for the magnetic interactions of the perturbed state are obtained by neglecting the effect of the perturbation on the Coulomb exchange and onsite Coulomb repulsion, in which case the spin-orbit effects are contained within a hopping term that conserves m_s but not necessarily m_j. As before, we will consider the two-site, two-orbital case. When written in the perturbed basis, the Hamiltonian contains, respectively, the anisotropic hopping term, a Coulomb exchange term, and an onsite Coulomb repulsion term:

$$\mathcal{H} = \sum_{\langle ij\rangle}(\mathbf{c}_i^\dagger \cdot \mathbf{T}_{ij} \cdot \mathbf{c}_j + h.c.) + \sum_{\substack{m_j, m_j' \\ \langle ij\rangle}} K_{ij} c_{i,m_j}^\dagger c_{j,m_j'}^\dagger c_{j,m_j} c_{i,m_j'} + U\sum_i c_{i,\uparrow}^\dagger c_{i,\uparrow} c_{i,\downarrow}^\dagger c_{i,\downarrow}, \tag{2}$$

where

$$\mathbf{c}_i = \begin{pmatrix} c_{i,\uparrow} \\ c_{i,\downarrow} \end{pmatrix} \tag{3}$$

and $c_{i,\uparrow}^\dagger$ ($c_{i,\downarrow}^\dagger$) creates an electron in the perturbed SOMO at the ith site, with $m_j = +\frac{1}{2}$ ($-\frac{1}{2}$). The notation $\langle ij\rangle$ indicates a summation over nearest neighbors. The 2×2 matrix $\mathbf{T}_{ij}$ is given by

$$\mathbf{T}_{ij} = t_{00}^{ij}\mathbf{I}_{2\times 2} + \frac{1}{2}\sum_{\mu=\{x,y,z\}} C_{00,\mu}^{ij}\sigma_\mu, \tag{4}$$

where t_{ab}^{ij} is the transfer integral between unperturbed a and b orbitals at sites i and j, respectively; $\mathbf{I}_{2\times 2}$ is the two-dimensional identity matrix, σ_μ is a Pauli matrix, and C_{00}^{ij} is Moriya's SO-mediated transfer parameter given by

$$C_{00,\mu}^{ij} = \lambda\sum_{a,b}\frac{\langle 0_i|\hat{L}_\mu^i|a_i\rangle}{\epsilon_a - \epsilon_0}t_{a0}^{ij} + t_{0b}^{ij}\frac{\langle b_j|\hat{L}_\mu^j|0_j\rangle}{\epsilon_b - \epsilon_0}. \tag{5}$$

Just as in the absence of spin-orbit coupling, in the large-U limit, the hopping is treated as a perturbative correction to the energy. Up to second order, the resulting effective-spin Hamiltonian is given by

$$\mathcal{H}_{ij} = -\mathcal{J}_{ij}\,\hat{\mathbf{S}}_i\cdot\hat{\mathbf{S}}_j + \mathbf{D}_{ij}\cdot(\hat{\mathbf{S}}_i\times\hat{\mathbf{S}}_j) + \hat{\mathbf{S}}_i\cdot\Gamma_{ij}\cdot\hat{\mathbf{S}}_j, \tag{6}$$

where

$$\mathcal{J}_{ij} = 2K_{ij} - \frac{4t_{00}^{ij\,2}}{U} + \sum_\mu\frac{|C_{00,\mu}^{ij}|^2}{U}, \tag{7}$$

$$[\mathbf{D}_{ij}]_\mu = \frac{2i}{U}\left(C_{00,\mu}^{ij}t_{00}^{ji} - t_{00}^{ij}C_{00,\mu}^{ji}\right), \tag{8}$$

$$[\Gamma_{ij}]_{\mu,\nu} = \frac{1}{U}\left(C_{00,\mu}^{ij}C_{00,\nu}^{ji} + C_{00,\mu}^{ji}C_{00,\nu}^{ij}\right). \tag{9}$$

The first term in the Hamiltonian represents the isotropic exchange interaction. The second term, for which $\mathbf{D}_{ij}$ is a vector, represents the antisymmetric Dzyaloshinsky-Moriya (DM) interaction. The third term, for which Γ_{ij} is a symmetric rank-two tensor, gives rise to the anisotropic exchange (AE), which is responsible for the splitting of the triplet manifold.

We limit our analysis of the anisotropic interactions to those between nearest neighbors in a single π-stack. Given the fairly one-dimensional structure of **1** and **2**, these intrastack interactions are expected to dominate over the corresponding interstack interactions. The presence of this crystallographic mirror plane bisecting each π-stack provides that

$C^{ij,\pi}_{00,x} = C^{ij,\pi}_{00,y} = 0$. In order to see this, we discuss the symmetry of the matrix elements in Eq. (5). The local angular momentum operators $\hat{L}^i_\mu, \hat{L}^j_\mu$ transform as A'', A'', and A' for $\mu = x, y$, and z, respectively. The unperturbed SOMOs on each radical, that is, $|0_i\rangle, |0_j\rangle$, are of A'' symmetry. The requirement that nonzero matrix elements must transform as A' provides some restrictions on $C^{ij}_{00,\mu}$:

(i) $C^{ij,\pi}_{00,\mu}$ is only nonzero for orbitals $|a_i\rangle, |b_j\rangle$ that transform as A''; otherwise, t^{ij}_{a0}, t^{ij}_{0b} would vanish.

(ii) As a result, $C^{ij,\pi}_{00,\mu}$ is only nonzero for $\mu = z$ since the matrix elements $\langle 0_i|\hat{L}^i_{x,y}|a_i\rangle, \langle b_j|\hat{L}^j_{x,y}|0_j\rangle$ transform as $A'' \otimes A'' \otimes A'' = A''$ and therefore vanish.

Given these symmetry considerations, $\mathbf{D}_{ij}$ must be normal to the mirror plane bisecting sites i, j. For antiferromagnetic alignment, canted moments are therefore preferred to lie within the mirror plane, that is, the molecular xy-plane. For ferromagnetically aligned spins, this result also dictates that the AE interaction favors alignment of spins in the same plane. As discussed below, this implies easy-axis anisotropy in **1** and **2**, in the context of the crystallographic symmetry. The results here are thus in exact agreement with the results obtained by considering the mixing of the $\mathcal{T}_z$ and $\mathcal{S}^{(0)}$ states. In local coordinates, the interaction between nearest neighbors in a π-stack is therefore

$$\mathcal{H}^\pi_{ij} = -\left(2K^{ij}_{00} + \frac{|C^{ij,\pi}_{00,z}|^2 - 4{t^{ij}_{00}}^2}{U}\right)\hat{\mathbf{S}}_i \cdot \hat{\mathbf{S}}_j + \frac{4iC^{ij,\pi}_{00,z}t^{ij}_{00}}{U}(\hat{S}_{i,x}\hat{S}_{j,y} - \hat{S}_{i,y}\hat{S}_{j,x}) + \frac{2|C^{ij,\pi}_{00,z}|^2}{U}\hat{S}_{i,z}\hat{S}_{j,z}. \quad (10)$$

The order of magnitude of these terms has been estimated previously for **1**.[11] Of particular note is the exceptionally small value of $t^{ij}_{00} \sim 0.01$ eV, due to the near orthogonal overlap of neighboring SOMOs discussed above.[9,10] The transfer integrals t^{ij}_{a0} that determine the magnitude of $C^{ij,\pi}_{00}$ are not so constrained; we estimate these to be much larger than t^{ij}_{00}, on the order of 0.1 eV. For **1**, the molecular spin-orbit coupling constant λ can be represented in terms of the atomic value for selenium (0.1 eV),[26] and $\Delta\epsilon = \epsilon_a - \epsilon_0$ can be taken to be 1 eV. Thus, the value of $|C^{ij}_{00}|$ can be estimated as $\lambda t^{ij}_{a0}/\Delta\epsilon \sim 0.01$ eV. Based on these values, and taking $U \sim 0.8$ eV from electrochemical measurements,[6] both the second (DM) and third (AE) terms in Eq. (10) are found to be $\sim 10^{-4}$ eV. Extending this approach to the mixed S/Se variant **2**, and approximating λ as the average of the atomic SO constants of the selenium and sulfur,[26] leads to an estimated reduction in the value of $|C^{ij}_{00}|$ by a factor of about 0.6 (see Table I). This qualitative conclusion compares well with the results obtained by FMR measurements.

III. FMR STUDIES

In order to probe the magnetic anisotropy of **1** and **2**, we have measured electron spin resonance (ESR) spectra at low temperature, a technique that is sensitive to the bulk magnetic excitations (spin waves) of the ferromagnetically ordered phase.[27] This technique has been employed in the study of various organic materials including charge-transfer salts,[28,29] doped fullerenes,[30] and radicals.[31,32]

TABLE I. Magnetic and spin-orbit parameters.

	1	**2**
T_C (K)[a]	17	12.8
H_c (Oe)[a]	1370 (2 K)	250 (2 K)
H_A (Oe)[a]	8200 (5 K)	3100 (4 K)
λ_{avg} (eV)[b]	0.116	0.069
$\sim |C^{ij,\pi}_{00}|$ (eV)	0.022	0.014

[a]Data from Ref. 6.
[b]Based on values in Ref. 26.

In a typical single-crystal experiment, microwave radiation is applied to a sample at a set frequency, and the energies of magnetic excitations are tuned using an external field $\mathbf{H}_{ext}$ that can be varied in magnitude and direction with respect to the crystal. Since the dimensions of the crystal are much smaller than the wavelength of the radiation, only $k = 0$ spin waves are usually excited. Whenever the energy of such spin waves matches the frequency of applied radiation, resonant absorption is observed.

The angular dependence of the transmission spectra for the mixed S/Se radical **2** is shown in Figs. 6 and 7.[33] The polar angle θ_H gives the angle between $\mathbf{H}_{ext}$ and the crystallographic c-axis, while ϕ_H is the azimuthal angle. As with analogous studies of **1**, reported previously in Ref. 11, the variation of

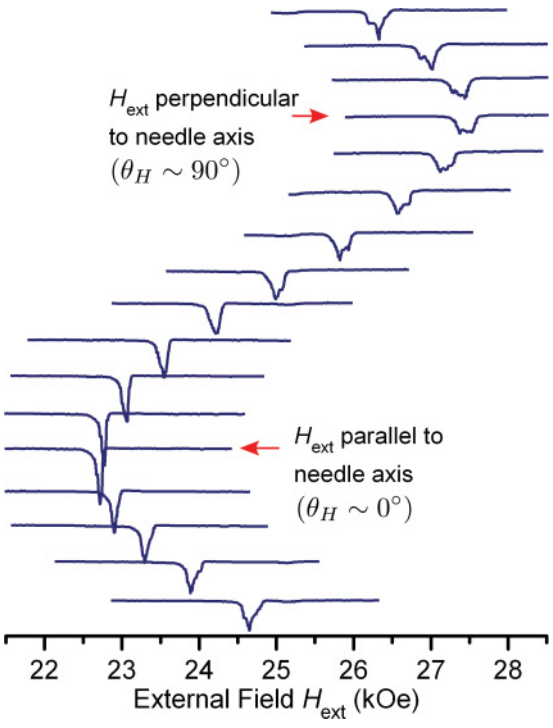

FIG. 6. (Color online) Transmission spectra for **2** as a function of polar angle θ_H for $\omega = 73$ GHz and $T = 2$ K. The needle axis and crystallographic c-axis are approximately equivalent. The resonance for $\mathbf{H}_{ext} \parallel c$-axis ($\theta_H = 0°$) is sharp and consists of a single peak, whereas the resonance for $\mathbf{H}_{ext} \perp c$-axis ($\theta_H = 90°$) is broad and multipeaked.

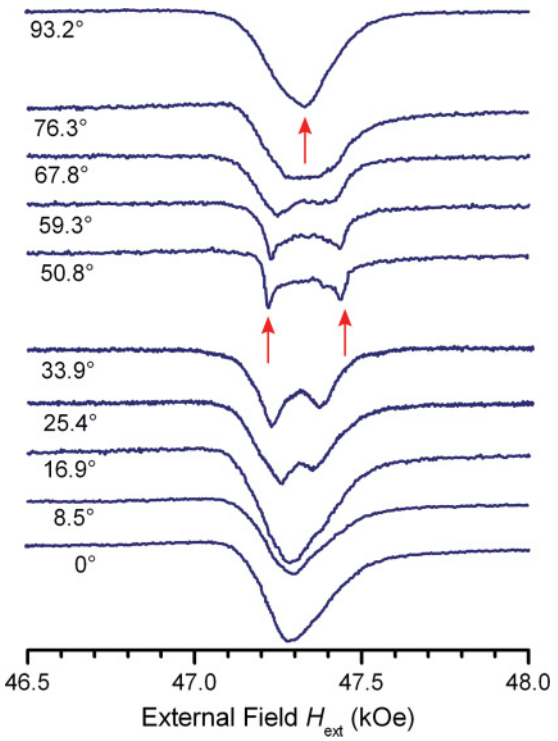

FIG. 7. (Color online) Transmission spectra for **2** as a function of azimuthal angle ϕ for $\mathbf{H}_{ext} \perp c$-axis ($\theta_H = 90^\circ$) and $\omega = 127$ GHz. The average position of the resonance is constant, suggesting little anisotropy in the ab-plane, but a splitting is observed with period of $\Delta\phi_H = 90^\circ$. The relationship between the experimental ϕ_H angle and the crystal axes is unknown, although the results imply $\phi_H = 0^\circ$ corresponds to $\mathbf{H}_{ext} \,||\, a$- or b-axis (see discussion).

the resonance field with θ_H is indicative of easy-axis magnetic anisotropy with an easy c-axis. For **2**, a slight splitting of the resonance was also observed for $\theta_H \neq 0^\circ$, the magnitude of which is periodic in ϕ_H with a maximum on the order of 300 Oe, as shown in Fig. 7 for $\mathbf{H}_{ext}$ oriented in the ab-plane. Evidence of a similar splitting can be observed in the lineshapes of **1**. However, the magnitude of the splitting does not exceed 100 Oe, making resolution difficult.

It is tempting to associate this splitting with the presence of magnetically inequivalent sites. Indeed, in the context of the crystal, the interactions given in Eq. (10) establish four different orientations for the $\mathbf{D}_{ij}$ within the unit cell, providing four magnetically inequivalent π-stacks (see Fig. 5). Stacks (sublattices) related by a twofold axis ($\bar{4}^2$) possess identical local easy planes, but $\mathbf{D}_{ij}$ vectors that are antiparallel while stacks related by a $\bar{4}$ or $\bar{4}^3$ operation possess orthogonal local easy planes. This latter observation explains the easy crystallographic c-axis, as alignment of spins parallel to this axis is the only orientation that allows all spins to lie within their local easy plane while satisfying the ferromagnetic interstack exchange. In this sense, the angular dependence of the resonance properties of both **1** and **2** can be expected to resemble closely those of a uniaxial ferromagnet. Indeed, the appearance of the hysteresis curves for these materials closely resembles those predicted for this case.[34]

Accordingly, we consider the resonance properties of **1** and **2** in the context of exchange-coupled, but magnetically inequivalent, π-stacks by modifying the results obtained by Tomita for the paramagnetic resonance of exchange-coupled spins.[35] Based on this approach, we identify and discuss three regimes:

(i) In the absence of exchange coupling between the stacks, the magnetic excitations of the crystal are exactly the one-dimensional $k = 0$ spin waves of the individual stacks. For a given sublattice labeled by χ, the excitation energy of this mode is given by the expectation value of the Hamiltonian

$$\mathcal{H}_\chi = \sum_{\langle ij \rangle} \mathcal{H}^{\pi}_{ij,\chi} + \sum_i g\mu_B \, \mathbf{S}^{\chi}_i \cdot \mathbf{H}_{ext} \tag{11}$$

and can generally be determined by the usual Holstein-Primakoff approach.[27] Here, we have ignored the anisotropy of the g tensor. For a collinear spin arrangement, the AE term is the only contributor to the $k = 0$ spin-wave energy, implying two experimentally distinct sublattices with orthogonal easy planes. In this regime, the spectra of **1** and **2** would display two distinct resonances with an energetic separation $\langle \Delta\mathcal{H} \rangle_{k=0}$, corresponding to the excitation of spin waves in these two sublattices. It can be shown that whenever ϕ_H measured from the a-axis is a multiple of 90° or $\theta_H = 0^\circ$, the spin waves become degenerate, and the resonances would coalesce into a single peak. This general angular dependence agrees with the experiment, but the magnitude of splitting observed is far less than predicted in the absence of exchange.

(ii) For the opposite case, when the magnitude of interstack exchange coupling ($\sim \mathcal{J}_\perp$) far exceeds $\langle \Delta\mathcal{H} \rangle_{k=0}$, only a single "exchange amalgamated" resonance will be observed, representing a bulk, sublattice averaged spin wave. The position of this resonance can be predicted based on the expectation value of the average Hamiltonian $\bar{\mathcal{H}} = 1/4 \sum_\chi \mathcal{H}_\chi$.

(iii) In the intermediate regime, as $\mathcal{J}_\perp \sim \langle \Delta\mathcal{H} \rangle_{k=0}$, the resonance properties will display aspects of both previously discussed regimes. That is, a resonance should be found centered at the same position as in (ii), but slightly split, with a reduced peak separation compared with (i). The results of Tomita suggest the onset of splitting should occur for $\mathcal{J}_\perp \lesssim 2\langle \Delta\mathcal{H} \rangle_{k=0}$, allowing for an approximate comparison of the isotropic intrastack and anisotropic interstack interactions in **1** and **2**.

Following from the above discussion, approximate resonance conditions were obtained from a model coarse-grained Hamiltonian with anisotropic intrastack interactions that are an average over the four sublattices in the crystal (see Appendix for details). Within this approximation, the expected response is exactly that of a uniaxial easy-axis ferromagnet with an easy c-axis and spin-wave gap due to spin-orbit effects given by $|C|^2/U$ at $H_{ext} = 0$. The resonance frequency is given by

$$\omega = \gamma \left\{ \begin{array}{c} \left[H_{ext} \cos(\theta - \theta_H) + \frac{H_A}{2}(3\cos^2\theta - 1) \right]^2 \\ - \left[\frac{H_A}{2} \sin^2\theta \right]^2 \end{array} \right\}^{\frac{1}{2}}, \tag{12}$$

where θ is the angle between the total magnetization $\mathbf{M}$ and the c-axis, θ_H is the angle between $\mathbf{H}_{ext}$ and the c-axis, and $\gamma = \bar{g}\mu_B/\hbar$ is the average gyromagnetic ratio of the radicals. The anisotropy field H_A at zero temperature is given by

$$H_A = \frac{1}{\gamma\hbar} \frac{\left| C^{ij,\pi}_{00} \right|^2}{U}. \tag{13}$$

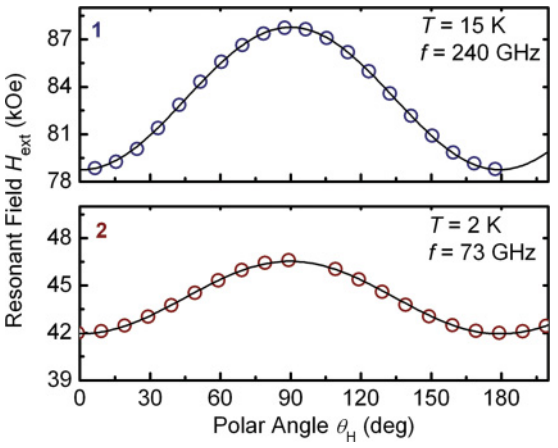

FIG. 8. (Color online) Angular dependence of the resonance field $H_{\rm ext}$ for **1** and **2** at high frequency. Where splitting of the resonance is observed, the average position of the two peaks is displayed. The black curves are a fit of Eq. (14). Data for **1** reproduced from Ref. 11.

The coarse-grained model predicts that the average resonance position is independent of the azimuthal angle ϕ_H, in correspondence with the experimental observations. At high frequency, such that $H_{\rm ext}$ and $\omega/\gamma \gg H_A$, then $\theta = \theta_H$ for all orientations, and the approximate angular dependence of the resonance field can be written as

$$H_{\rm ext} \approx \frac{\omega}{\gamma} - \frac{H_A}{2}(3\cos^2\theta_H - 1) + \frac{H_A^2\gamma}{8\omega}\sin^4\theta_H, \quad (14)$$

where the $\sin^4\theta_H$ term represents only a small correction. The experimental angular dependence of the resonance field at high frequency for **1** and **2** indeed conforms to a predominantly $\cos^2\theta_H$ dependence prescribed by Eq. (14) (Fig. 8). These results identify both **1** and **2** as uniaxial ferromagnets with an easy c-axis.

For $\mathbf{H}_{\rm ext}$ || c-axis (θ,$\theta_H = 0$), the resonance frequency reduces to

$$\omega = \gamma(H_{\rm ext} + H_A). \quad (15)$$

The temperature dependence of H_A for **2** was determined by a fit of Eq. (15) to data collected at three different frequencies (72.7, 104.6, and 128.8 GHz). Data for **1** were taken from Ref. 11. The results show the onset of anisotropy at temperatures about 10 K above the respective ordering temperatures of **1** and **2**. As the temperature is decreased, H_A continues to rise, having values of 8.2 kOe (at 5 K) for **1** and 3.1 kOe (at 4 K) for **2** at the lowest measured temperatures (see Fig. 9). Based on these results, approximate values for $|C_{00}^{ij,\pi}|$ were estimated and found to agree well with the anticipated order of magnitude, that is, ~0.01 eV (see Table I). The difference in the measured anisotropy of **1** and the mixed S/Se **2** is well explained by spin-orbit effects; the ratio of the measured $|C_{00}^{ij,\pi}|$ values is 0.6, in accordance with the prescribed value.

The results also allow $|C_{00}^{ij,\pi}|^2/U$ to be estimated as 7 and 3 K for **1** and **2**, respectively. Broken-symmetry density functional theory (DFT) estimates of $\mathcal{J}_\perp$ for **2** suggest both the isotropic and anisotropic interactions are of similar magnitude.[9] Indeed, our explanation for the splitting of the resonance of **2** requires that $\mathcal{J}_\perp$ is the same order as $|C_{00}^{ij,\pi}|^2/U$. In the case of **1**, enhancement of the lateral isotropic exchange may reduce the splitting, but nonetheless the ordering temperature of 17 K suggests that the isotropic interactions do not significantly exceed the 7 K anisotropic terms. This observation highlights the importance of considering spin-orbit effects, which should not be assumed to be small in heavy-atom organic magnets.

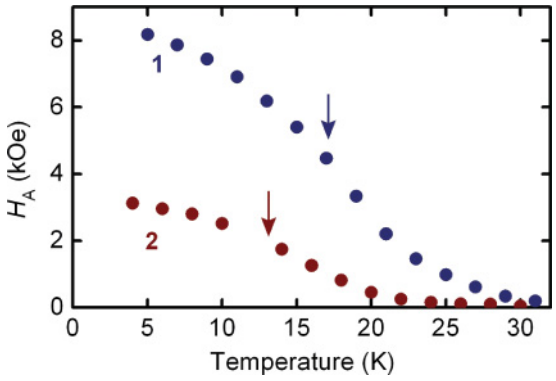

FIG. 9. (Color online) Temperature dependence of the anisotropy field H_A for **1** and **2**. The ferromagnetic ordering temperatures T_C = 12.8, 17 K for **1** and **2**, respectively, are indicated by an arrow. Data for **1** reproduced from Ref. 11.

IV. CONCLUSION

We have previously proposed that the magnetic anisotropy in **1** must arise from spin-orbit effects rather than from magnetic dipolar interactions, which alone could not account for the observed magnitude of H_A.[11] In this investigation, the observation that the anisotropy is a function of the S/Se content in isostructural radicals offers further evidence for this conclusion. Since the magnitude of dipolar anisotropy depends only on crystal structure and morphology, it can not explain the different magnitude of anisotropy for **1** and **2**. Detailed analysis of the anisotropic exchange, on the other hand, suggests that it accounts for both the magnitude and uniaxial character of the magnetic anisotropy.

The results of this study provide a compelling explanation for the origin of the coercive fields H_c observed for **1** and **2**, which far exceed the coercive fields observed in light-atom organic magnets. Experimental H_c values scale with the intrinsic anisotropy field H_A, which for the present compounds is large due to spin-orbit effects associated with the heavy Se atom. Furthermore, it has been demonstrated that the strength of this anisotropic exchange is similar to the strength of the isotropic magnetic interactions, reaffirming the importance of considering spin-orbit effects on the magnetic properties of heavy-atom organic materials.

In our analysis, we discussed the importance of both molecular and crystallographic symmetry in determining the effect of the anisotropic exchange. We believe we have demonstrated conclusively the universality of Moriya's anisotropic exchange: that it can be found for both metal- and nonmetal-based heavy-atom magnets. We hope that the detailed analysis presented here will provide a basis for the future study of spin-orbit effects in other nonmetal-based magnetic materials,

and unify the interpretation of magnetic phenomena in d-, f-, and p-block materials.

ACKNOWLEDGMENTS

We thank the NSERC (Canada) and the US NSF (Grants No. DMR0804408 and No. CHE-0924374) for financial support. S.M.W. acknowledges the NSERCC for a Graduate Scholarship. The NHMFL is supported by the NSF (DMR-0654118) and by the State of Florida.

APPENDIX

Neither the isotropic nor DM interactions contribute to the $k = 0$ spin-wave gap, and so can be ignored in the calculation of the resonance conditions. In local coordinates, the AE Hamiltonian for the four sublattices is given by

$$\mathcal{H}^{\pi}_{ij,\chi} = \frac{2\left|C^{ij,\pi}_{00}\right|^2}{U}\hat{S}^{\chi}_{i,z}\hat{S}^{\chi}_{j,z}, \tag{A1}$$

where $\chi = \{A,B,C,D\}$ label the four sublattices represented in the crystallographic unit cell (see Fig. 5). Written in terms of the crystallographic directions, the spin operators are

$$\hat{S}^{A}_{i,z} = \frac{1}{\sqrt{2}}\left(\hat{S}^{A}_{i,a} + \hat{S}^{A}_{i,b}\right), \tag{A2}$$

$$\hat{S}^{B}_{i,z} = \frac{1}{\sqrt{2}}\left(\hat{S}^{B}_{i,a} - \hat{S}^{B}_{i,b}\right), \tag{A3}$$

$$\hat{S}^{C}_{i,z} = \frac{1}{\sqrt{2}}\left(-\hat{S}^{C}_{i,a} - \hat{S}^{C}_{i,b}\right), \tag{A4}$$

$$\hat{S}^{D}_{i,z} = \frac{1}{\sqrt{2}}\left(-\hat{S}^{D}_{i,a} + \hat{S}^{D}_{i,b}\right), \tag{A5}$$

where a,b refer to the corresponding crystallographic directions.

The coarse-graining procedure employed is to write the approximate Hamiltonian as $\bar{\mathcal{H}} \approx \frac{1}{4}\sum_{\chi}\mathcal{H}_{\chi}$ and to drop the sublattice label χ on the spin operators ($\hat{S}^{\chi}_{i,a} \rightarrow \hat{S}_{i,a}$). The resulting coarse-grained AE Hamiltonian is then given by

$$\mathcal{H} = \sum_{\langle ij\rangle}\frac{\left|C^{ij,\pi}_{00}\right|^2}{U}(\hat{S}_{i,a}\hat{S}_{j,a} + \hat{S}_{i,b}\hat{S}_{j,b}). \tag{A6}$$

Finally, since $\hat{\mathbf{S}}_i \cdot \hat{\mathbf{S}}_j = \hat{S}_{i,a}\hat{S}_{j,a} + \hat{S}_{i,b}\hat{S}_{j,b} + \hat{S}_{i,c}\hat{S}_{j,c}$, this can be rewritten as

$$\mathcal{H} = \sum_{\langle ij\rangle}\frac{\left|C^{ij,\pi}_{00}\right|^2}{U}(\hat{\mathbf{S}}_i \cdot \hat{\mathbf{S}}_j - \hat{S}_{i,c}\hat{S}_{j,c}), \tag{A7}$$

where the additional isotropic component does not affect the $k = 0$ spin-wave gap.

*oakley@uwaterloo.ca
†shill@magnet.fsu.edu

[1] M. Kinoshita, P. Turek, M. Tamura, K. Nozawa, D. Shiomi, Y. Nakazawa, M. Ishikawa, M. Takahashi, K. Awaga, T. Inabe, and Y. Maruyama, Chem. Lett. **20**, 1225 (1991).
[2] M. Tamura, Y. Nakazawa, D. Shiomi, K. Nozawa, Y. Hosokoshi, M. Ishikawa, M. Takahashi, and M. Kinoshita, Chem. Phys. Lett. **186**, 401 (1991).
[3] R. Chiarelli, M. Novak, A. Rassat, and J. L. Tholence, Nature (London) **363**, 147 (1993).
[4] A. Alberola, R. J. Less, C. M. Pask, J. M. Rawson, F. Palacio, P. Oliete, C. Paulsen, A. Yamaguchi, R. D. Farley, and D. M. Murphy, Angew. Chem. Int. Ed. **42**, 4782 (2003).
[5] P. Day, Nature (London) **363**, 113 (1993).
[6] C. M. Robertson, A. A. Leitch, K. Cvrkalj, R. W. Reed, D. J. T. Myles, P. A. Dube, and R. T. Oakley, J. Am. Chem. Soc. **130**, 8414 (2008).
[7] L. Beer, J. L. Brusso, A. W. Cordes, R. C. Haddon, M. E. Itkis, K. Kirschbaum, D. S. MacGregor, R. T. Oakley, A. A. Pinkerton, and R. W. Reed, J. Am. Chem. Soc. **124**, 9498 (2002).
[8] C. M. Robertson, D. J. T. Myles, A. A. Leitch, R. W. Reed, D. M. Dooley, N. L. Frank, P. A. Dube, L. K. Thompson, and R. T. Oakley, J. Am. Chem. Soc. **129**, 12688 (2007).
[9] C. M. Robertson, A. A. Leitch, K. Cvrkalj, D. J. T. Myles, R. W. Reed, P. A. Dube, and R. T. Oakley, J. Am. Chem. Soc. **130**, 14791 (2008).
[10] A. A. Leitch, S. M. Winter, R. A. Secco, P. A. Dube, and R. T. Oakley, J. Am. Chem. Soc. **131**, 7112 (2009).
[11] S. M. Winter, S. Datta, S. Hill, and R. T. Oakley, J. Am. Chem. Soc. **133**, 8126 (2011).
[12] R. C. Haddon, Nature (London) **256**, 394 (1975).
[13] P. Lahti, Adv. Phys. Org. Chem. **45**, 93 (2011).
[14] I. Ratera and J. Veciana, J. Chem. Soc. Rev. **41**, 303 (2012).
[15] L. Beer, J. L. Brusso, R. C. Haddon, M. E. Itkis, H. Kleinke, A. A. Leitch, R. T. Oakley, R. W. Reed, J. F. Richardson, R. A. Secco, and X. Yu, J. Am. Chem. Soc. **127**, 18159 (2005).
[16] J. Hubbard, Proc. R. Soc. London, Ser. A **276**, 238 (1963).
[17] C. J. Calzado, J. Cabrero, J. P. Malrieu, and R. Caballol, J. Chem. Phys. **116**, 2728 (2002).
[18] O. Kahn, *Molecular Magnetism* (VCH, New York, 1993).
[19] O. Kahn, J. Galy, Y. Journaux, J. Jaud, and I. Morgenstern-Badarau, J. Am. Chem. Soc. **104**, 2165 (1982).
[20] M. Mito, Y. Komorida, H. Tsuruda, J. S. Tse, S. Desgreniers, Y. Ohishi, A. A. Leitch, K. Cvrkalj, C. M. Robertson, and R. T. Oakley, J. Am. Chem. Soc. **131**, 16012 (2009).
[21] D. Dai, H. Xiang, and M.-H. Whangbo, J. Comput. Chem. **29**, 2187 (2008).
[22] A. V. Pivtsov, L. V. Kulik, A. Y. Makarov, and F. Blockhuys, Phys. Chem. Chem. Phys. **13**, 3873 (2011).
[23] The DM interaction is only required to vanish between sites related by an inversion center. In centric space groups, weak ferromagnetism may occur by canting of spins on sites not related by an inversion center provided the overall state respects inversion symmetry. See I. Dzyaloshinsky, J. Phys. Chem. Solids **4**, 241 (1958).
[24] T. Moriya, Phys. Rev. **120**, 91 (1960).
[25] T. Yildirim, A. B. Harris, A. Aharony, and O. Entin-Wohlman, Phys. Rev. B **52**, 10239 (1995).
[26] M. Blume and R. E. Watson, Proc. R. Soc. London, Ser. A **271**, 565 (1963).

[27]S. V. Vonsovskii, *Ferromagnetic Resonance* (Pergamon, New York, 1966).
[28]C. Coulon and R. Clerac, Chem. Rev. **104**, 5655 (2004).
[29]M. Dumm, A. Loidl, B. Alavi, K. P. Starkey, L. K. Montgomery, and M. Dressel, Phys. Rev. B **62**, 6512 (2000).
[30]D. Arcon, P. Cevc, A. Omerzu, and R. Blinc, Phys. Rev. Lett. **80**, 1529 (1998).
[31]T. Kambe, K. Kajiyoshi, K. Oshima, M. Tamura, and M. Kinoshita, Polyhedron **24**, 2468 (2005).
[32]J. M. Rawson, A. Alberola, H. El-Mkami, and G. M. Smith, J. Phys. Chem. Solids **65**, 727 (2004).
[33]Single crystals of the mixed S/Se radical **2** were prepared by electrochemical reduction described previously (Ref. 6). Orientation and temperature-dependent FMR studies were performed on these single crystals at multiple frequencies (70–130 GHz) using a superheterodyne cavity-based spectrometer developed around a Quantum Design Physical Property Measurement System (PPMS) configured with a 7 T split-pair magnet; this spectrometer is described in detail elsewhere (see Refs. 36 and 37).
[34]E. C. Stoner and E. P. Wohlfarth, Philos. Trans. R. Soc. London A **240**, 599 (1948).
[35]K. Tomita, M. Tanaka, T. Kawasaki, and K. Hiramatsu, Prog. Theor. Phys. **29**, 817 (1963).
[36]M. Mola, S. Hill, P. Goy, and M. Gross, Rev. Sci. Instrum. **71**, 186 (2000).
[37]S. Takahashi and S. Hill, Rev. Sci. Instrum. **76**, 023114 (2005).